Materials Science & Engineering A 598 (2014) 154–161

Contents lists available at ScienceDirect

Materials Science & Engineering A

journal homepage: www.elsevier.com/locate/msea

Tensile behaviors and deformation mechanisms of a nickel-base single crystal superalloy at different temperatures

X.G. Wang, J.L. Liu, T. Jin *, X.F. Sun

Superalloys Division, Institute of Metal Research, Chinese Academy of Sciences, Shenyang 110016, China

ARTICLE INFO

Article history:
Received 8 October 2013
Received in revised form
26 November 2013
Accepted 1 January 2014
Available online 8 January 2014

Keywords:
Tensile behaviors
Stress jump
Dislocation structure
Stacking faults
Single crystal superalloy

ABSTRACT

The tensile behaviors of an experimental nickel-base single crystal superalloy have been studied from room temperature to 1100 °C. Obvious work hardening during the tensile tests from room temperature to 760 °C has been observed. In contrast, at 900 °C and 1000 °C only a slight work hardening occurs. Furthermore, by using transmission electron microscopy (TEM), the microstructures of the alloy after tensile tests at various temperatures have been investigated. Detailed analysis demonstrates the stacking faults (SFs) presented in the γ matrix at room temperature, 600 °C and 760 °C, which were seldom reported previously. These stacking faults are responsible for the appearance of stress jump (named steps) on the stress–strain curves. On the other hand, these stacking faults effectively prevent slipping of the dislocations and have a great contribution to work hardening. Apart from that, the stacking faults in γ′ precipitates from room temperature to 900 °C have also been observed. The interfacial dislocation networks at 1000 °C and 1100 °C cause a weak resistance to the slip dislocations because of the high flow stress. The $a/3\langle 121\rangle$ and $a/2\langle 011\rangle$ type dislocations are of vital importance for plastic deformation and rupture of the experimental alloy. At last, the relation between deformation mechanisms and tensile behaviors has been reasonably explained.

1. Introduction

Nickel-base single crystal superalloys are widely used for manufacturing aircraft engine turbine blades due to their excellent mechanical and corrosion resistance properties at elevated temperatures. The outstanding resistance to creep and fatigue follow from a unique two-phase equilibrium microstructure, which consists of an ordered gamma-prime (γ′, Ni_3Al) precipitates with $L1_2$ structure coherently embedded in a gamma (γ) austenitic phase [1–3]. The mechanical behaviors and the deformation mechanisms of superalloys are significantly influenced by the morphology of the γ′ phase. Consequently, modifying the alloy chemical compositions and heat treatment to control the size, volume fraction and distribution of γ′ precipitates is effective to obtain optimal comprehensive performance for the alloy [4,5]. The experimental alloy used in this work is a fourth generation Ru-containing single crystal superalloy, which contains the elements of Co, Re, Ta and W. By adding these transition elements into the alloy, the strength of the γ disordered solid solution can be enhanced, while the stacking fault energy can be reduced. Thus the mechanical properties are improved [6,7], e.g. the tensile yield strength of the single crystal superalloys. The maximum yield strength of the PWA 1480 and SRR99 superalloys is at 760 °C [8,9], while for the CMSX-4 superalloy [10] and the experimental superalloy used in this work are about 800 °C and 900 °C, respectively.

Tensile test is a basic test for many metal materials and the results are significant reference for creep and fatigue. Tensile tests of many single crystal superalloys have been carried out [11–14], while the fourth generation superalloys are rarely reported and the mechanisms leading to their outstanding properties are still incompletely understood. The stacking faults present in γ matrix at room temperature, 600 °C and 760 °C have been rarely reported previously; however, they have a significant influence on the mechanical behaviors. In order to further study the relationship between temperature and deformation mechanisms, a series of tensile tests at different temperatures was carried out. The results of the experiments reported here are aimed at elucidating the deformation mechanisms at different temperatures.

2. Experimental

The alloy used in this study is a Ru-containing single crystal superalloy. The nominal chemical compositions of the alloy in weight percent is as follows: 12Co, 4Cr, 1Mo, 6W, 5.4Re, 3Ru, 6Al, 8.4Ta, and the balance of nickel. The master alloy was melted in a vacuum induction furnace and casted as a 9 kg-ingot. The single crystal rods were directionally solidified along the [001] direction

* Corresponding author. Tel.: +86 24 2397 1757.
E-mail address: tjin@imr.ac.cn (T. Jin).

0921-5093/$ - see front matter © 2014 Elsevier B.V. All rights reserved.
http://dx.doi.org/10.1016/j.msea.2014.01.001

at a constant withdrawal rate of 6 mm/min using the Bridgman method. After that, the as-cast rods were cut to short bars of about 68 mm in length. The heat treatment was carried out on the experimental alloy as follows:

1315 °C, 16 h+1325 °C, 16 h+AC→1150 °C, 4 h+AC→870 °C, 24 h+AC (AC: air cooling).

Here, it should be noted that the two-step solution heat treatment is supersolvus heat treatment. After heat treatment, the metallographic sample was mechanically polished and etched in a solution of 20 g $CuSO_4$+100 ml HCl+5 ml H_2SO_4+80 ml H_2O. The morphology of the two phases was observed by an Inspect F50 field emission scanning electron microscope (FESEM). The volume fraction and size of γ′ precipitates were measured and calculated using the Image-Pro Plus software (the γ′ precipitates observed here are all re-precipitating from the solid solution). The cylindrical specimens of tensile test have gauge length and diameter of 25 mm and 5 mm, respectively. The tensile tests were carried out on an AG-250KNE mechanical test machine at room temperature (RT), 600 °C, 760 °C, 900 °C, 1000 °C and 1100 °C with a constant strain rate of 1.67×10^{-3} s^{-1} along the [001] direction to rupture. A three-region resistance furnace was adopted to heat the specimens with a temperature fluctuation less than ±5 °C.

After the tensile tests, the foils for transmission electron microscopy (TEM) observation were cut perpendicular to the [001] direction and 5 mm apart from the fracture. After mechanically grinding to about 50 μm, these thin foils were electrochemically thinned in a solution of 10 ml perchloric acid and 90 ml ethanol at a current of 30 mA and temperature of −25 °C. As a result of the presence of the porosity in the specimens, final thinning was carried out by ion milling at an angle of 4° and voltage of 3.5 kV for 5–10 min. The microstructures of all specimens were examined using a JEM 2100 TEM operating at 200 kV.

3. Results and discussion

3.1. Tensile behavior

Fig. 1 shows the tensile engineering strain–stress curves at different temperatures. The experimental alloy exhibits different tensile behaviors at different temperatures. An obvious work hardening takes place at room temperature, 600 °C and 760 °C. At room temperature, some stress jumps (steps in Fig. 1 inset) appear in the wake of a well-defined yield point. By contrast, the steps at 600 °C are wider than those at room temperature and no well-defined yield point appears on the curve. The flow stress at room temperature and 600 °C dramatically increases in a step type. In fact, there is a short increasing stage of flow stress before the steps appear. These phenomena mentioned above might be correlated with the dislocation multiplication and formation of the stacking faults in the γ matrix. Detailed analysis will be done in Section 3.3.2. At 900 °C, the flow stress quickly drops to a platform after exceeding the upper yield point. There is a slight work hardening taking place at 1000 °C after a well-defined yield point. Because of the high temperature, the flow stress at 1100 °C gradually decreases after yield point until rupture.

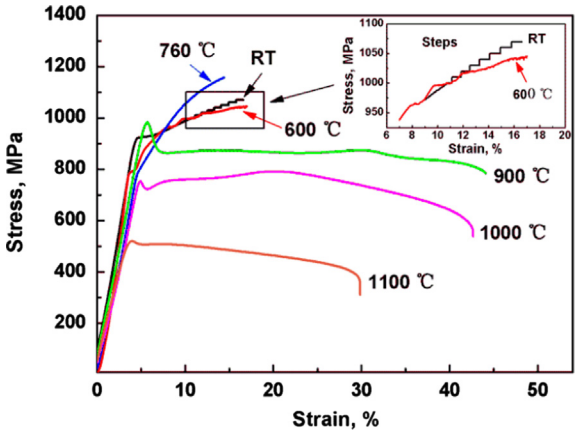

Fig. 1. Tensile engineering strain–stress curves of the experimental alloy at different temperatures. Inset is the partial enlargement of the steps at room temperature and 600 °C.

Fig. 2 demonstrates the temperature dependence on tensile strength and plasticity of the experimental alloy. The yield strength, as is shown in Fig. 2a, almost remains the same from room temperature to 760 °C, and then gradually increases with the increasing temperature and reaches a maximum at 900 °C. After that it drops dramatically. The ultimate tensile strength gradually decreases from room temperature to 600 °C, then increases with temperature increasing and reaches its maximum at 760 °C. The trend of the ultimate tensile strength above 760 °C is similar to the yield strength above 900 °C as shown in Fig. 2a. The trend of the tensile plasticity of the alloy in Fig. 2b is as follows: the percentage elongation remarkably decreases from room temperature to 760 °C and reaches a minimum at 760 °C. After that it dramatically increases and reaches a maximum at 900 °C, and then decreases by a large margin. The trend of the percentage of reduction of area is similar to percentage elongation. In comparison, the percentage of reduction of area reaches its minimum and maximum at 600 °C and 1000 °C, respectively.

3.2. Microstructural evolution

The microstructure of the alloy after heat treatment and the statistical results of γ′ size are shown in Fig. 3. The segregation of refractory elements in dendrite core is significantly reduced after 32 h solution heat treatment. During the following aging heat treatment, the γ′ phase re-precipitates from the γ solid solution and grows into regular cuboids, as shown in Fig. 3a. According to the statistical results, the average size of the γ′ cuboids in dendrite and interdendritic regions are almost the same, while the size in dendrite core is more uniform. The volume fraction of the γ′ phase is about 70% and the average size of the γ′ cuboids is about 0.3 μm (the standard deviation is 0.066 μm) as shown in Fig. 3b.

Fig. 4 demonstrates the deformation microstructure of the experimental alloy after tensile test at room temperature. Some straight dislocations in the γ′ precipitates are observed. Morphologically, this type of dislocations all lie in the [010] direction and are only about 0.1 μm in length, which manifests that they are in a steeply inclined state. TEM analysis demonstrates that these dislocations are the $a/3\langle121\rangle$ type dislocations lying in the {111} plane in the γ′ precipitate while at $g=0\bar{2}0$ type operating vector the stacking faults are invisible.

Some stacking faults present both in the γ matrix channels and the γ′ precipitates. The formation of the stacking faults during tensile test at room temperature is unusual, and what interests us more is that the stacking faults present in the γ matrix, which are rarely reported before. It indicates that the stacking fault energy of the experimental alloy is very low. After observing many other TEM images with the same operating conditions, we find that there are more stacking faults in the γ matrix channels of the [010] direction than those in the [100] direction, which means that the [010] and [100] channels in different stress states. The main reason for the different stress states is that the direction of the specimen axis deviates from the ideal [001] direction (within 10°). Consequently, the crystal rotation will interrupt the equivalence between the [100] and [010] matrix during tensile test, then the shear stress in the two directions of matrix is different from each other. Additionally, taking